

# APPLICATION PROSPECTS OF VTEM™ HELICOPTER TIME-DOMAIN ELECTROMAGNETICS IN CHINA

PRESENTED AT SEG GEM CHENGDU, CHINA, 2015

**Yan Luo**  
ARCN

**Lin Zhu**  
ARCN

**Zhao Zhao**  
ARCN

**Zhiao Han**  
Geotech Ltd.

**Shaolin Lu**  
Geotech Ltd.

**Jean M. Legault**  
Geotech Ltd.

## SUMMARY

VTEM™ helicopter time-domain EM systems have recently been introduced in China in 2013 for mineral exploration. Results from recent survey over a polymetallic Pb-Zn deposit in Inner Mongolia are presented in plan and modeled in cross-section. Its high conductance and low magnetic susceptibility signature can be used to guide exploration for similar Pb-Zn deposits in the region, as well as elsewhere in China.

## INTRODUCTION

Airborne electromagnetics (AEM) is a fast and efficient exploration method that has rapidly developed over the last several decades (Annan, 2013; Fountain, 2008; Thomson et al., 2007; Macnae, 2007). More recently, AEM systems, in particular helicopter time-domain EM (HTEM), have continued to be developed and been widely applied with significant effect, becoming one of the most important means of ore and groundwater prospecting around the world (Vallée et al., 2011; Allard, 2007).

AEM was developed early but slowly in China (Lei et al. 2006) and Chinese-made ATEM systems are still currently in the testing stages (Chen, 2012). With the increasing difficulty related to mineral resource exploration, a fast and effective exploration method is urgently needed in China.

The helicopter-borne VTEM (Versatile Time Domain Electromagnetic; Witherly et al., 2004; Prikhodko et al., 2010) is one of the leading HTEM systems in the world that has recently been introduced in China. It features a large dipole moment and high signal to noise ratio that provides superior depth of investigation (Killeen, 2014).

In 2013, a VTEM test survey over a known polymetallic lead-zinc volcanogenic massive sulfide (VMS) deposit was carried out in Xinjiang Province, China in cooperation with ARCN and XNGEB (Luo, et al., 2014). It demonstrated that the method can detect and resolve high conductance targets such as VMS deposits and had great potential for deep exploration in China. Based on this successful test, a VTEM survey was carried out in 2014 over a known Pb-Zn deposit in Heilongjiang and Inner Mongolia, China, the results which are described in this study.

## GEOLOGY AND MINERALIZATION

The geotectonic position of this known Pb-Zn deposit is in the Duolun anticlinorium, Wendurmiao-Wengniute Caledonian geosyncline fold belt of Inner Mongolia's central geosyncline fold system. Harhada group of Wendurmiao and shallow metamorphic rock series of Permian age are the outcropping strata in this deposit. Banded marble of Harhada group is the main host rock and the plagiogranite has a close relationship with the mineralization. Coarse grained galena and sphalerite are the major metallic minerals of the sulfide ores.

## VTEM SYSTEM

The VTEM system is a geophysical instrument that has been in continuous development since its inception in 2002 (Prikhodko et al., 2010). There are currently three configurations of the VTEM helicopter HTEM system, based on transmitter (Tx) loop diameter and dipole-moment (NIA), which are designed to cover a variety of geologic targets and survey environments (Killeen, 2014): the lightweight VTEM (18m Tx loop, 240,000 NIA), the high powered VTEM MAX (35m loop, 1,300,000 NIA) and the versatile VTEM PLUS system (Figure 1 and Table I) which is likely the most widely deployed HTEM instrument throughout the world and is currently being used in China.

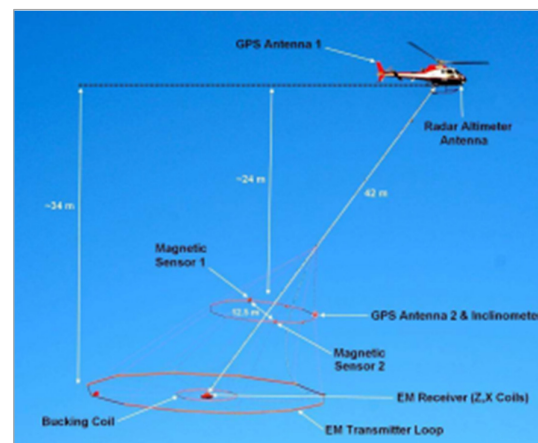


Figure 1: VTEM PLUS system configuration.

VTEM PLUS features a coincident-coplanar, vertical dipole transmitter-receiver configuration which produces a symmetric system response. Any asymmetry in the measured EM profile is due to conductor dip, not the

system or direction of flight. This allows for easy identification of the conductor location and for interpretation of the EM data. The low noise receiver in combination with the high power transmitter yields a system that has one of the best signal to noise ratios among available airborne systems.

**Table 1:** VTEMLUS system specifications.

<b>Transmitter</b>	
Transmitter-receiver geometry	In-loop, coincident-coplanar vertical dipole
Transmitter coil	Dodecagon shape-vertical axis, 26m diameter x 4 turns (2124m <sup>2</sup> area)
Base frequency	Standard 30Hz or 25Hz depending on powerline
Pulse shape	Polygonal
Pulse width	Typically 43% of the half cycle-over 7ms in length
Peak dipole moment	Up to 625,000NIA(400,000 typical)
Peak current	Up to 310 Amperes(200 typical)
<b>Receiver</b>	
Coils	Standard Z & X, optional Y (113m <sup>2</sup> & 19.7m <sup>2</sup> area)
Sample rate	192kHz over entire waveform
Bandwidth	Up to 50kHz
Spheric noise rejection	Digital
Industrial noise rejection	60Hz or 50Hz
Time-Gates	0.096-8.083ms (Ch. 14-46)
<b>Magnetometer</b>	
Type	Geometrics G822A (Horizontal gradiometer optional)
<b>Mechanical</b>	
Nominal survey speed	90km/hr
EM transmitter/receiver ground clearance	30-40m

VTEMLUS has been designed to detect and discriminate between moderate to excellent conductors using a low base frequency, long pulse width, and derived B-field EM measurement. The B-field is derived by integrating dB/dt time-domain EM data collected at 192kHz over the entire wave-form.

## VTEM SURVEY RESULTS

In 2014, a VTEM survey test was carried out over a known Pb-Zn mineral deposit in Inner Mongolia. Three (3) lines were flown at 500m spacings directly above the deposit. Figure 2 shows the planned lines and the deposit outline.

There is a strong response on two test lines respectively in the VTEM dB/dt Z-component decay profiles, and a weaker one on the third line (Figure 3). The characteristic double-peak anomalies in the VTEM profiles indicate that the conductive body is relatively thin and dips at a steep angle approximately orthogonal to the line-direction. Weakening amplitudes to the southeast indicate SSE plunge or limited strike-length. The late-channel behaviour (red-colored pro-files visible) indicates good conductivity-thickness for the central conductor. Other VTEM anomalies along the line that are limited to earliest time-gates (only blue profiles visible) and do not extend into late-channels are consistent with near-surface overburden-responses.

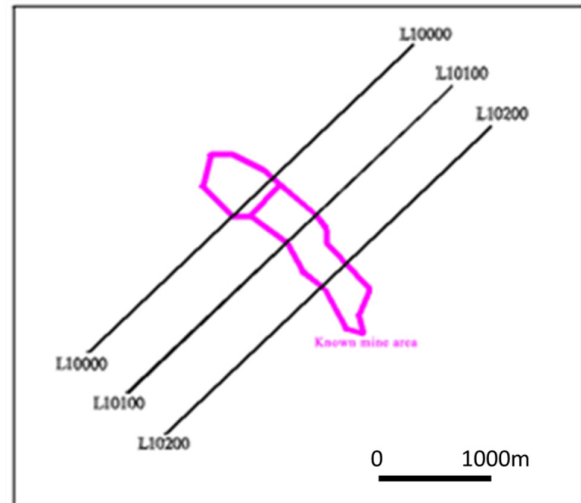


**Figure 2:** Planned flight lines over the known Pb-Zn deposit.

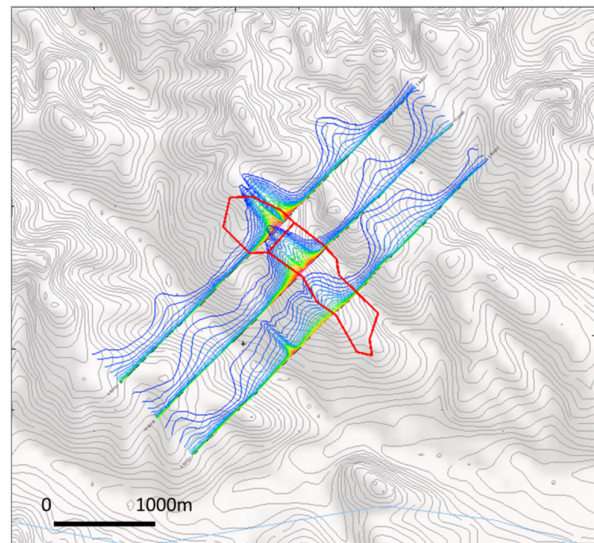


**Figure 3:** VTEM dB/dt Z-Component profiles and deposit outline.

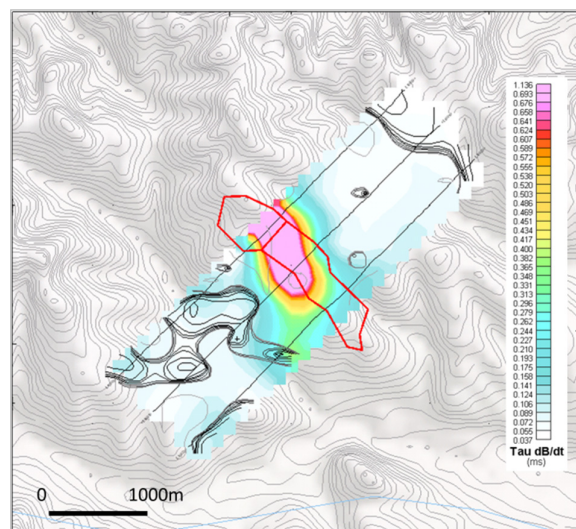


**Figure 4:** TAU map and CVG contours, with deposit outline.

The VTEM dBz/dt time-constant (Tau) map in Figure 4 was obtained using sliding window method, where Tau's are calculated using the least-squared fit of a straight-line (log/linear space) over the last 4 available gates above the noise-level. Figure 4 highlights the area of elevated Tau (>1.1msec) that is consistent with high conductivity and clearly coincides with the Pb-Zn deposit outline. Since Tau is relatively insensitive to depth of burial, the rapid weakening along the south-easternmost profile suggests that the Pb-Zn deposit pinches or is possibly mined-out.

Figure 5 presents the total magnetic intensity (TMI) contour across the test area. Along with the calculated vertical magnetic gradient (CVG) contours in Figure 4, they show a low magnetic intensity anomaly over the known mineral deposit. This likely reflects a combination of magnetite-depletion due to hydrothermal alteration surrounding the deposit and the typically low magnetic susceptibilities of lead and zinc sulfides within the orebody.

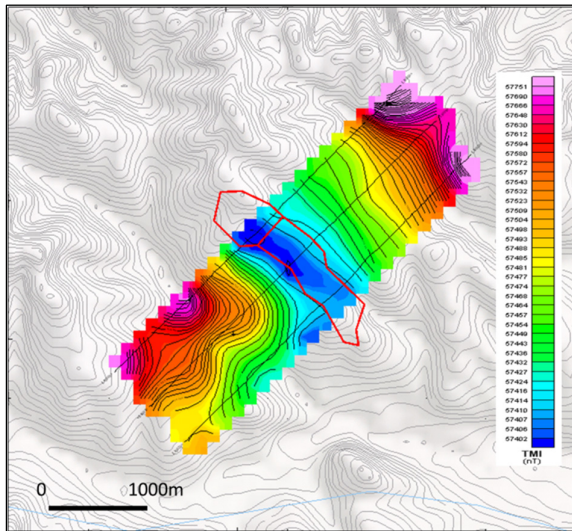


Figure 5: TMI colour image and contours, with deposit outline.

This polymetallic deposit rich in Pb-Zn is therefore characterized by high conductivity and low magnetic susceptibility based on the analysis of these VTEM survey results. These multiparameter signatures should be useful in the search for similar undiscovered deposits with these characteristics in the surrounding area.

### VTEM PLATE MODELING

The VTEM results have been further analyzed using Maxwell™ (EM Interpretation Technology, Midland, AUS) 3D conductive plate modeling. Figure 6 shows the observed and model profiles for line 10000 that is situated over the strongest part of the VTEM anomaly. Also shown is the RDI resistivity-depth image section that is based on the 1D apparent resistivity vs. depth calculation of Meju (1998) along with the outline of the modeled plate. The depth-of-investigation is shown to exceed 450m.

Figure 7 shows the Maxwell plate modeling for L10000. The results indicate that the 100m x 350m thin conductive plate is buried at 25m, dips steeply at 83° SW, and has a conductance of 120 siemens, which is consistent with lead-

zinc orebodies that are typically moderately-conductive (i.e., Caber deposit; Prikhodko et al., 2010).

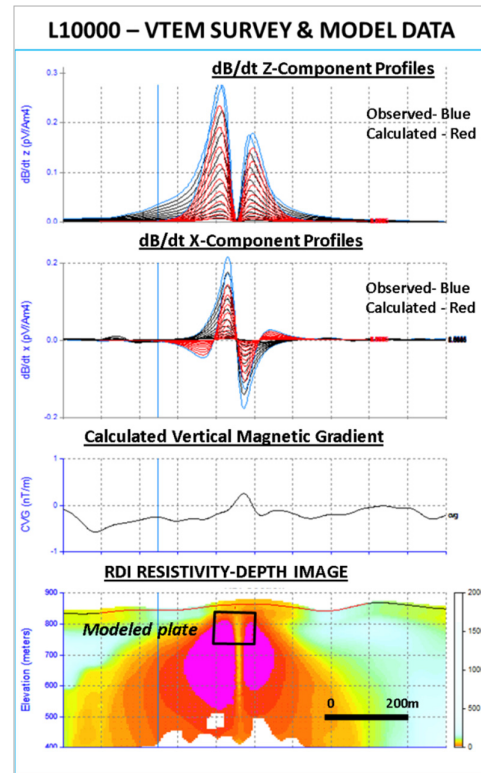
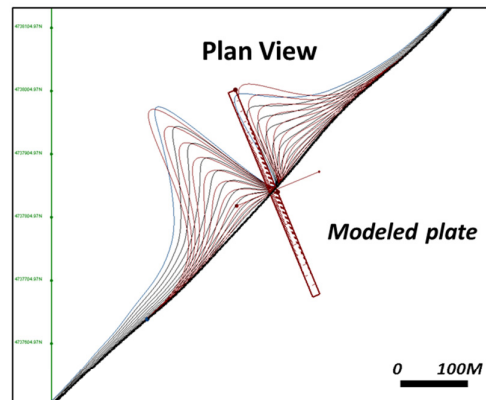


Figure 6: L10000 VTEM Maxwell plate-modeling results and RDI resistivity-depth image, showing 3D outline of modelled plate.

### L10000 – VTEM MAXWELL™ PLATE MODEL



Target Plate Parameters		
Parameter	Value	Units
Depth	-25	Meters
Dip	83	Degrees
Dip Direction	247.5	Degrees
Rotation	0	Degrees
Length	350	Meters
Depth Extent	100	Meters
Conductivity-Thickness	120	Siemens
Depth—depth from surface to top-center of the plate		

Figure 7: L10000 VTEM Maxwell plate-modeling results.

## CONCLUSIONS

VTEM surveys have the benefits of typically short duration, relatively low cost per line-km, small terrain effects, high efficiency and large depth of investigation, leading to effective exploration. After two years testing and survey production, VTEM surveys have achieved remarkable results in China. Our Pb-Zn case-study shows that ATEM surveys are worth applying for exploration of polymetallic deposits and should help promote the future application of helicopter time-domain EM in China.

## REFERENCES

Allard, M., 2007, On the origin of the HTEM species, in B. Milkereit, ed., Proceedings of the Fifth Decennial International Conference on Mineral Exploration, 355-374.

Annan, P., 2013, Airborne EM – Lessons learnt and future opportunities: 13th SAGA Biennial Conference and Exhibition, and 6<sup>TH</sup> International AEM Conference and Exhibition, Conference proceedings, 36-37.

Chen, S.-D., 2012, Response calculation and ground-loop calibration of helicopter transient electromagnetic system, PhD thesis, Jilin University.

Fountain, D., 2008, 60 years of airborne EM – focus on the last decade: 5<sup>TH</sup> International Conference on Airborne Electromagnetics, Expanded abstracts, 8 p.

Killeen, P., 2014, Exploration Trends and Developments in 2013: The Northern Miner, 30 p.

Lei, D., Hu, X.-Y., and Zang, S.-F., 2006, Development status quo of airborne electromagnetic: Contributions to Geology and Mineral Resources Research, 2006-01.

Luo, Y., Zeng, Y., Shi, Y., Yang, B., Li, B.-H., and Zheng, Q.-S., 2014, The test of airborne transient electromagnetic technology in the volcanics-associated massive sulfide district: Geophysical and Geochemical Exploration, **38**, 842-845.

Macnae, J., 2007, Developments in broadband airborne electromagnetics in the past decade, in B. Milkereit, ed., Proceedings of Exploration 07: Fifth Decennial International Conference on Mineral Exploration, 387-398

Meju, Maxwell A., 1998, A simple method of transient electromagnetic data analysis: Geophysics, **63**, 405-410.

Prikhodko, A., Morrison, E., Bagrianski, A., Kuzmin, P., Tishin, P., and Legault, J. M., 2010, Evolution of VTEM – technical solutions for effective penetration: 21<sup>ST</sup> Geophysical Conference and Exhibition, ASEG, Extended abstracts, 1-5.

Thomson, S., D. Fountain, and T. Watts, 2007, Airborne geophysics — Evolution and revolution, in B. Milkereit, ed., Proceedings of Exploration 07: Fifth Decennial International Conference on Mineral Exploration, 19-37.

Vallée, M.A., Smith, R. S., and Keating, P., 2011, Metalliferous mining geophysics – State of the art after a decade in the new millennium: Geophysics, **76**, W31-W50.

Witherly, K., Irvine, R., and Morrison, E.B., 2004, The Geotech VTEM time domain electromagnetic system: SEG, Expanded abstracts, 1217-1221.